Review of Scientific Instruments

RESEARCH ARTICLE | APRIL 01 1995

Ultrahigh sensitivity single-photon detector using a Si avalanche photodiode for the measurement of ultraweak biochemiluminescence

Ultrahigh sensitivity single-photon detector using a Si avalanche photodiode for the measurement of ultraweak biochemiluminescence

Takashi Isoshima; Yasushi Isojima; Katsuhiko Hakomori; ... et. al

Check for updates

Rev Sci Instrum 66, 2922–2926 (1995)
https://doi.org/10.1063/1.1145578

CrossMark

View Online

Export Citation

Articles You May Be Interested In

Intracellular simulated biophoton stimulation and transsynaptic signal transmission

Appl. Phys. Lett. (November 2022)

Advanced research equipment for fast ultraweak luminescence analysis

Rev Sci Instrum (September 2003)

Audio acoustic modeling using full-wave methods

J Acoust Soc Am (May 2008)

Downloaded from http://pubs.aip.org/aip/rsi/article-pdf/66/4/2922/8809475/2922_1_online.pdf

AIP Publishing

Ultrahigh sensitivity single-photon detector using a Si avalanche photodiode for the measurement of ultraweak biochemiluminescence

Takashi Isoshima
Frontier Research Program, The Institute of Physical and Chemical Research (RIKEN), 2-1 Hirosawa, Wako, Saitama 351-01, Japan

Yasushi Isojima
Institute for Protein Research, Osaka University, 3-2 Yamadaoka, Suita, Osaka 565, Japan

Katsuhiko Hakomori
Fujitsu Limited, 1015 Kamikotanaka, Nakahara-ku, Kawasaki, Kanagawa 211, Japan

Kazuro Kikuchi
Department of Electronic Engineering, Faculty of Engineering, The University of Tokyo, 7-3-1 Hongo, Bunkyo-ku, Tokyo 113, Japan

Katsuya Nagai and Hachiro Nakagawa
Institute for Protein Research, Osaka University, 3-2 Yamadaoka, Suita, Osaka 565, Japan

(Received 29 June 1994; accepted for publication 1 December 1994)

A single-photon detector using a Si avalanche photodiode (APD) has been constructed. A *trans*-impedance type front-end circuit was employed in order to achieve a high signal-to-noise ratio. The APD and front-end circuit were cooled in liquid nitrogen to reduce dark count rate and circuit noise. The system performances were measured, and the achieved dark count rate and total quantum efficiency were 0.08 count/s and 5%, respectively. The sensitivity was evaluated to be of the order of 10^{-19} W. The APD single-photon detector was demonstrated to be available for measurement of the ultraweak biochemiluminescence at the order of 10^{-19} W/mm^2 from brain slices, i.e., hippocampal slices. It was shown that the addition of tetrodotoxin to the hippocampal slice caused a decrease in the intensity of biochemiluminescence. © *1995 American Institute of Physics.*

I. INTRODUCTION

Recently, the necessity of the single-photon counting method for ultraweak light detection has been increasing in many research fields on physics, chemistry, and life sciences, as well as optical communications. Among its applications, detection of the biochemiluminescence, i.e., the spontaneous ultraweak light emission on the order of 10^{-15} W/cm^2 or less from all kinds of living organisms, seems one of the most challenging ones. The ultraweak biochemiluminescence is thought to be related to functional activities such as oxidative stress[1] and respiratory activity,[2] and their increases reflect those in the metabolic rate.[3] It is also known that in a brain slice the metabolic rate is related to the neural activity: a high potassium condition or electric stimulation increases respiratory activity.[4] Therefore, the ultraweak biochemiluminescence is expected to be used as a noninvasive probe for important biological functions like neural activities.

As a detector for the single-photon counting method, a semiconductor avalanche photodiode (APD) is attracting a lot of attention. Compared with a conventional photoelectron multiplier tube (PMT), the APD has many advantages such as a lower operating voltage, compactness, high intrinsic quantum efficiency, and longer detectable wavelength.[5–7] On the other hand, it has a few disadvantages such as a smaller average multiplication factor, larger excess noise, and usually a higher dark count rate. The large excess noise originates in the avalanche multiplication process, and is recognized in the single-photon counting method as a quite different probability distribution of multiplication factor for each photogenerated carrier compared with a PMT. The probability distribution in an APD with reverse bias less than the breakdown voltage is a monotonously decreasing function of multiplication factor,[8–10] in contrast with the distribution in a PMT which has a maximum at about the average multiplication factor. Therefore most of the avalanche-amplified signal is masked with the electronic circuit noise, and the discrimination efficiency is usually less than 10% when the threshold for the pulse-height discrimination is settled so that almost all of the electronic circuit noise pulse is rejected. On the other hand, a lower discrimination threshold can be used to accept more avalanche-amplified pulses at the cost of a large increase in the dark-count rate due to the electronic circuit noise, e.g., total quantum efficiency of 25% at the dark-count rate of 100k count/s.[11] Another method to achieve high quantum efficiency is to use the Geiger mode operation[12–20] in which the APD is biased above the breakdown voltage and the breakdown triggered by a photogenerated or thermally generated carrier is quenched with an external circuit. High discrimination efficiency near unity is achievable when an APD with optimized structure, the so-called single-photon avalanche diode is employed.

In this paper, we demonstrate that very high sensitivity on the order of 10^{-19} W is achievable even with a single-photon detector using a nonselected sample of a commercially available Si APD for optical communication by cooling to liquid nitrogen temperature and optimizing the operating condition. We also describe the application of this

 0034-6748/95/66(4)/2922/5/$6.00 © 1995 American Institute of Physics

Alidouble Inc. v. TSMC Alidouble Ex. 2009, p. 2

Downloaded from http://pubs.aip.org/aip/rsi/article-pdf/66/4/2922/8809475/2922_1_online.pdf

system to the measurement of ultraweak biochemiluminescence on the order of 10^{-19} W/mm^2 from a cultured hippocampal slice consisting of neural and glial cells. This is, as far as we know, the first demonstration of availability of the APD photon counter to the ultraweak biochemiluminescence detection, and the first observation of ultraweak biochemiluminescence from a cultured cell group rather than the whole organism or homogenized tissue. In Sec. II, our Si APD single-photon detector system is described. In Sec. III, characterization of the system performances such as the total quantum efficiency and the dark count rate is described. In Sec. IV, application of the APD single-photon counter to the measurement of the ultraweak biochemiluminescence is described.

II. EXPERIMENT

The probability distribution of multiplication factor in an APD is quite different from that in a PMT, as mentioned previously. In the APD, the probability that a photogenerated carrier is multiplied m-fold decreases monotonously with the increase of m, and most of the photocurrent pulses are masked with the circuit noise. Therefore, the avalanche-amplified-signal-to-electronic-circuit-noise ratio at the front-end circuit must be as high as possible in order to achieve high discrimination efficiency. As long as the bandwidth of the system B is remarkably smaller than the intrinsic bandwidth of the avalanche pulse which is usually 1 GHz or more, the peak voltage of the signal pulse, V_{peak}, is proportional to the bandwidth, that is, $V_{\text{peak}} \propto BR_L$, where B is the bandwidth of the system and R_L is the load resistor to convert the photocurrent to the voltage. On the other hand, if the series noise is negligible and the dominant source of the parallel noise is R_L, the noise voltage is expressed as $V_{\text{noise,rms}} \propto (BR_L)^{1/2}$, and the signal-to-noise ratio is proportional to $(BR_L)^{1/2}$. Therefore, B and R_L should be designed as large as possible within the limit mentioned above for B. Since our front-end circuit is cooled to liquid nitrogen temperature, the assumption that the series noise is negligible and that the dominant source of the parallel noise is R_L, is acceptable. In order to make the contribution of the main amplifier noise further insignificant, we employed a *trans*-impedance-type front-end circuit. In a high-impedance buffer-type front-end circuit often used with APDs, the avalanche current pulse is first integrated on the total parasitic capacitance associated to the APD, to the input of the amplifier, and to R_L. In the *trans*-impedance-type front-end circuit, the pulse is integrated only on the parasitic capacitance associated to R_L and little affected by the capacitance of the APD and of the amplifier which is usually much larger than that of R_L. Therefore, the peak voltage of the signal pulse at the input of the main amplifier is much larger, and hence the contribution of the noise of the main amplifier is significantly smaller, than in cases where a high-impedance buffer is employed. Thus, the *trans*-impedance-type front-end circuit is preferable to the high-impedance buffer not only in the analog detection but also in the single-photon counting method.

Figure 1 shows the block diagram of the Si APD single-photon counting system.[11] The Si APD was a commercially available one (FPD08R32TX, Fujitsu, not a selected sample)

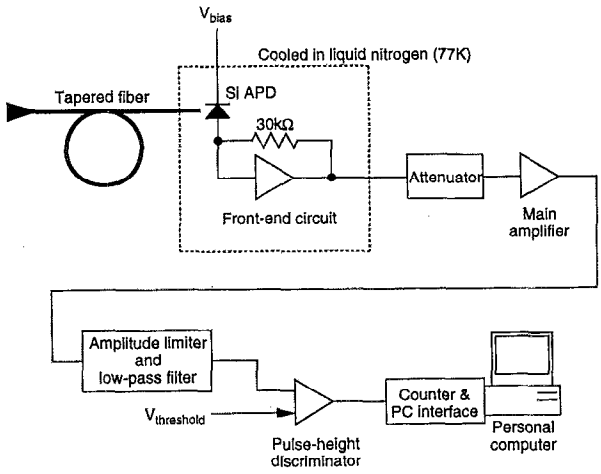

FIG. 1. Schematic diagram of the single-photon counting system. V_{bias} is the reverse bias voltage applied to the Si APD, and $V_{\text{threshold}}$ the threshold voltage for the pulse-height discrimination.

for optical communication, equipped with a FC-type optical fiber connector. The signal light was guided to the APD by a multimode optical fiber connected to the FC connector, which made the handling and optical alignment very easy. The custom-made optical fiber (Polymicro Technology Co.) was designed to have tapered input and output ends with diameters of 975 and 50 μm, respectively, which enabled us to detect light from a rather wide area with the APD of 50 μm diam. The APD was operated with reverse bias less than the breakdown voltage. The photocurrent pulses were converted to voltage pulses by the *trans*-inpedance-type front-end circuit, with which a wide bandwidth of 100 MHz and high *trans*-inpedance of 30 kΩ were achieved at the same time. The amplifier had three GaAs metal-semiconductor field-effect transistor amplifying stages and two emitter follower stages of Si bipolar transistors. The APD and front-end circuit were dipped directly into liquid nitrogen and cooled to a temperature of 77 K, in order to reduce the dark current of the APD and the thermal noise of the front-end circuit. The output of the front-end circuit was amplified with the main amplifier, the gain of which was optimized by the preceding attenuator. The amplitude limiter was employed in order to avoid saturation at the discriminator. In order to reduce the ringing of the pulses which might be caused by the poles of the front-end and main amplifier circuits at higher frequency, a fifth-order Thomson- (Bessel-) type low-pass filter of 63 MHz cutoff frequency was employed. Although the bandwidth could be limited directly at the front-end circuit, we preferred to use this fifth-order low-pass filter to reduce high frequency components significantly while maintaining a rather high cutoff frequency. The output of the pulse-height discriminator, which was ECL digital level, was connected to a personal computer interface which had a counter with an arbitrary presettable gate time. The result was read, recorded, and statistically analyzed by a personal computer. Because the system was ac coupled and small ringing at the end of a signal pulse was unavoidable, the interface circuit was designed to enable a "dead-time" sequence which inhibited us to count for a certain period

Downloaded from http://pubs.aip.org/aip/rsi/article-pdf/66/4/2922/8809475/2922_1_online.pdf

Alidouble Inc. v. TSMC
Alidouble Ex. 2009, p. 3

after a pulse was counted. The dead time was usually set to 3 μs, because the accompanied pulse caused by the ringing occurred about 2 μs after the "true" pulse.

We determined the optimal operating condition and characterized the system performance using a wavelength-variable light source, optical filters, and an optical power meter. Total quantum efficiency, i.e., efficiency to generate an output pulse for an incoming photon, and dark count rate were measured for characterization. The light source was a computer-controlled monochromator with a tungsten lamp (Metabolism Measurement Apparatus, Unisoku Co.). The monochromated light was guided by a bundle fiber, attenuated with optical filters, and guided to the Si APD by the tapered multimode fiber. The optical power spectrum of the wavelength-variable light source was calibrated with an optical power meter (TQ8210/TQ82014, Advantest Co.) at the output of the tapered fiber.

III. RESULTS

A. Optimal operating conditions

In order to achieve high total quantum efficiency and low dark count rate, the operating conditions must be optimized. To reject the electronic circuit noise pulses and accept only the avalanche-amplified pulses, the avalanche gain must be maximized and the avalanche-signal-to-electronic-noise ratio must be maximized, by adjusting the reverse bias voltage across the APD, V_{bias}. After maximization of the signal-to-noise ratio, the pulse-height discrimination threshold, $V_{threshold}$, should be set just above the noise level to reject almost all electronic noise pulses and to accept as many avalanche-amplified pulses as possible.

Although larger V_{bias} gives higher discrimination efficiency, semibreakdown can occur more easily. A semibreakdown pulse shows large, long, and very "noisy" shape, and thus causes multiple count for single pulse. Therefore, V_{bias} must be determined as the highest value without semibreakdown. Whether or not the multiple count occurs can be distinguished with the statistics of the count rate. The incoming of photons to the APD is a Poisson process, and thus the averaged count rate and its variant must be equal. If multiple count occurs, the variant becomes larger than the averaged count rate. Figure 2 shows the photon count rates and its statistical variants, as functions of V_{bias}. The measurements were made with the gate time of 1 s, and the averaged count rates and variants were obtained from 600 measurements for each value of V_{bias}. It can be seen that the variant is almost equal to the averaged count rate for V_{bias} of 57.50 V or less, while the variant is larger than the average for V_{bias} of 57.60 V or more. Thus, $V_{bias,opt}$, the optimal value of V_{bias}, was determined as 57.50 V. It should be noted that the breakdown voltage $V_{breakdown}$ of an APD depends on the temperature with the coefficient of 0.25%/K. Since $V_{breakdown}$ was around 57.8 V in our case, this temperature coefficient equals 0.14 V/K. Therefore, the temperature of the APD junction must be stabilized within about 0.1 K. We believe this condition was satisfied in our experiment, because the APD was dipped directly into liquid nitrogen and the power dissipation in the APD was sufficiently low because of the low counting rate.

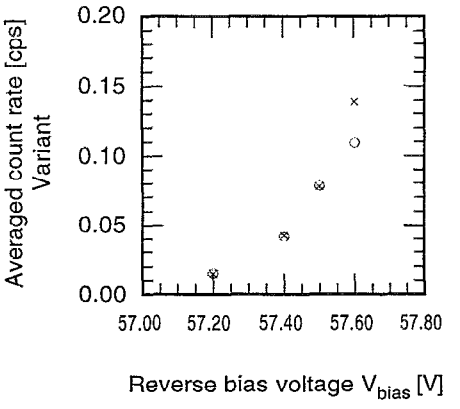

FIG. 2. Dependency of the averaged photon count rate and its variant on the reverse bias voltage V_{bias}. Open circles show the averaged count rate, and crosses show the variance.

Figure 3 shows the integral pulse-height distribution (rate of pulses exceeding the threshold) with and without incident light. These distributions are consistent with the fact that the pulse height due to circuit noise shows a Gaussian distribution and the probability decreases rapidly with the increase of pulse height while the probability for photocurrent pulses decreases slowly with the increase of pulse height.[8–10] Therefore, the count rate due to the electronic circuit noise can be reduced to almost zero while maintaining the rate due to the avalanche-amplified photocurrent signal. We determined to use the threshold level of 400 as optimal.

B. Total quantum efficiency

Figures 4(a) and 4(b) show the total efficiency as functions of wavelength. Figure 4(a) shows the total quantum efficiency at $V_{bias,opt}$ of the reverse bias voltage. Figure 4(b) shows those for $V_{bias,opt}$-0.30 V, $V_{bias,opt}$-0.10 V, $V_{bias,opt}$, $V_{bias,opt}$+0.10 V, and $V_{bias,opt}$+0.30 V. It can be seen that the total quantum efficiency increases with the increase of the bias voltage V_{bias}. It should be noted that the results for larger V_{bias} than $V_{bias,opt}$ are affected by the multiple count due to the semibreakdown. At $V_{bias,opt}$, total quantum effi-

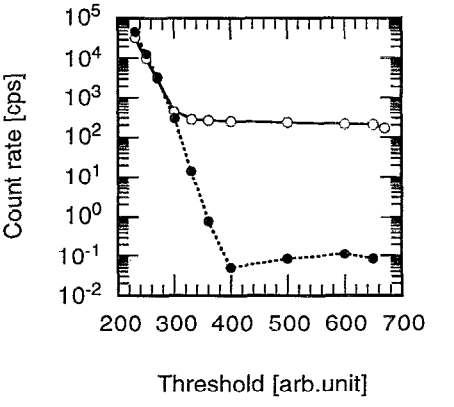

FIG. 3. Dependency of the single-photon count rate on the discriminating threshold level. Open circles and full line show the count rate with the incident light of 2.4×10^{-15} W at 850 nm, i.e., 1.0×10^4 incident photons per second. Closed circles and dotted line show the dark count rate.

Downloaded from http://pubs.aip.org/aip/rsi/article-pdf/66/4/2922/8809475/2922_1_online.pdf

Alicoable Inc. v. TSMC Alicoable Ex. 2009, p. 4

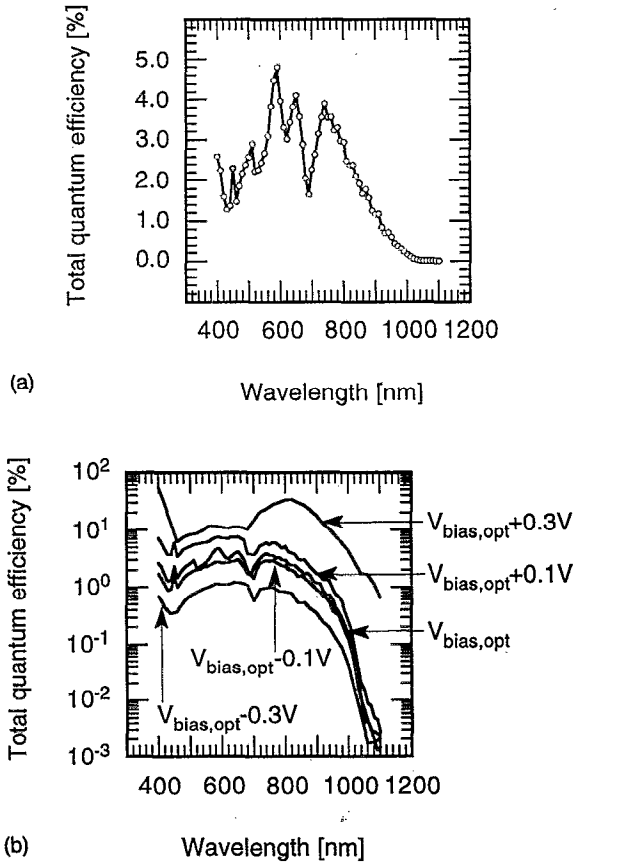

FIG. 4. (a) Dependency of the total quantum efficiency on the wavelength for the reverse-bias voltage of $V_{bias,opt}$. (b) Dependency of the total quantum efficiency on the wavelength for various reverse-bias voltages. The lines are for the reverse-bias voltage of $V_{bias,opt}+0.3$ V, $V_{bias,opt}+0.1$ V, $V_{bias,opt}$, $V_{bias,opt}-0.1$ V, and $V_{bias,opt}-0.3$ V from upper to lower trace, respectively. The optimal reverse-bias voltage $V_{bias,opt}$ was 57.50 V.

ciency of as high as 5% was obtained. Because the APD was cooled and the band gap of Si was widened, the spectrum of total quantum efficiency was shifted to a shorter wavelength compared with the quantum efficiency spectrum of an APD or photodiode at room temperature.

C. Dark count rate

The dark count rate at the optimal operating condition was 0.08 count/s (cps). This corresponds to the noise-equivalent power (NEP) of 1.1×10^{-19} W for 300 s measurements at the wavelength for the maximum total quantum efficiency, 590 nm. Figure 5 shows the NEP as a function of wavelength, which is expressed as

$$\mathrm{NEP}=\frac{h\nu}{\eta(\lambda)T}\sqrt{RT}$$

$$=\frac{hc_0}{\lambda\,\eta(\lambda)}\sqrt{\frac{R}{T}},$$

where $h\nu=hc_0/\lambda$ is the photon energy at a wavelength λ, c_0 is the speed of light in vacuum, h is the Planck's constant, $\eta(\lambda)$ is the total quantum efficiency at λ, $R=0.08$ cps is the dark count rate, and $T=300$ s is the count time used in the experiment described below. In this expression, the term for the fluctuation in the signal count is neglected[21] because the

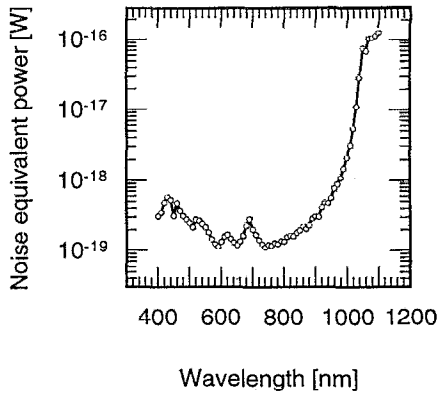

FIG. 5. Noise equivalent power as a function of wavelength for 300 s measurement under the optimal operating condition.

fluctuation in the dark counts are dominant under this measurement condition, $RT\gg1$. High sensitivity on the order of 10^{-19} W was achieved at a wide range of wavelengths from 400 to 1000 nm.

IV. APPLICATION TO THE ULTRAWEAK BIOCHEMILUMINESCENCE

Our research aims to apply this single-photon counting system to the measurement of ultraweak biochemiluminescence as a noninvasive probe for observation of activities in a cultured nucleus, a group of neural cells with a certain neural function. Preliminary experiments demonstrated that the ultraweak biochemiluminescence from a cultured hippocampal slice was observable, and that the intensity was modified by adding tetrodotoxin (TTX) which suppresses the neural activity.

A. Experiment

1. Tissue preparation and incubation

Male Normal Donryu rats, weighing 100–150 g, were decapitated without anesthesia. The cerebral hemispheres were rapidly removed and placed in an ice-cold medium (see below for the composition). The hippocampi were removed and transverse slices of 400 μm thickness were prepared using a microslicer (DTK-3000W, Dosaka EM Co.). The slices were moved on a porous (0.4 μm), transparent and low-protein-binding membrane (Millicell-CM, Millipore Co.) which was set in a small chamber with about 1 ml of volume.[22] The culture medium was Earle's Balanced Salt Solution (GIBCO), supplemented with $NaHCO_3$ (2.2 mg/ml), HEPES buffer (20 mM, pH 7.4) and glucose (final concentration: 6.5 mg/ml), and saturated with 95% O_2: 5% CO_2. The medium was recirculated under the membrane at a rate of 5 ml/min. The slices were preincubated for 2 h at 37 °C under dark condition before the photon counting procedure was started.

2. Photon counting of ultraweak biochemiluminescence from hippocampal slice

The tapered multimode optical fiber was placed at about 1 mm above the surface of the slice. The operating condition

Downloaded from http://pubs.aip.org/aip/rsi/article-pdf/66/4/2922/8809475/2922_1_online.pdf

Alidouble Inc. v. TSMC

Alidouble Ex. 2009, p. 5

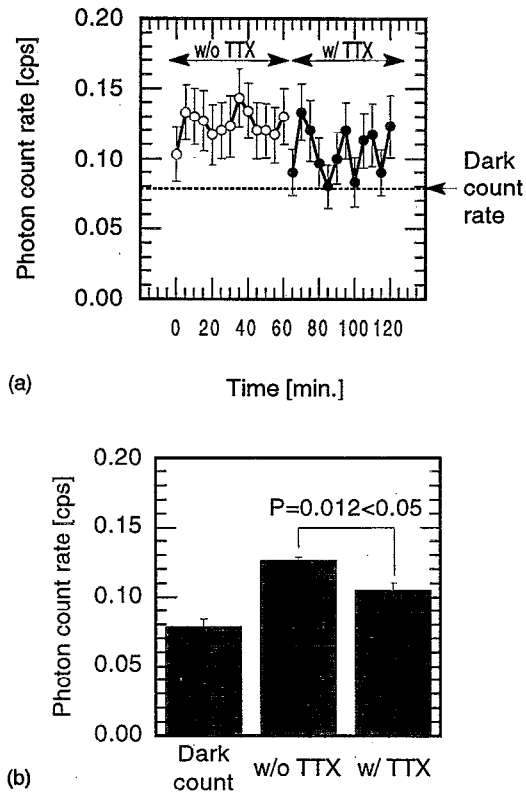

FIG. 6. (a) Changes in photon counting rate along with time. TTX was added at 60 min. Open and closed circles are the results before and after adding TTX, respectively. Standard errors are shown by error bars. The dark count rate measured without a slice is shown by dotted line. (b) Comparison of averaged single-photon counting rates. Standard errors are shown by error bars. The result of the T test ($P=0.012<0.05$) shows that the photon count rate after adding TTX is significantly smaller than that before adding TTX.

of the single-photon counter was set as optimal, i.e., threshold=400 and $V_{\text{bias}}=V_{\text{bias,opt}}$. Data were collected with the gate time of 1 s, and the averaged count rates and statistical variants were calculated from the data obtained in 5 min periods. Data exceeding 6 cps were omitted as multiple count due to the semibreakdown. During the measurement, the slice was incubated and the culture medium was circulated under the same condition as in the preincubation. After the measurement for 1 h as a control value, TTX (Sigma Co.) was added to the medium at the final concentration of 2 μM, and measurement was continued for another hour. In addition, the dark count rate was measured for 40 min without a slice.

B. Results

Figures 6(a) and 6(b) show the results of single-photon counting. The count rates obtained with and without the slice were 1.3×10^{-1} and 8×10^{-2} cps, respectively. Thus, the difference, 5×10^{-2} cps, was due to the biochemiluminescence from the hippocampal slice, and the intensity of it was evaluated on the order of 10^{-19} W/mm^2. It can be seen from Fig. 6(b) that the addition of TTX significantly reduced the intensity biochemiluminescence from hippocampal slice (1.3×10^{-1} cps before and 1.1×10^{-1} cps after the addition of TTX). TTX is known to suppress neural activity without killing cells, and our result suggests a close correlation between the neural activity and the biochemiluminescence. The culture condition was good enough to maintain the single-photon count rate for 4 h without adding TTX (data not shown).

[1] V. D. Antonenkov, Int. J. Biochem. **24**, 675 (1992).
[2] E. Hideg, M. Kobayashi, and H. Inaba, Biochim. Biophys. Acta **1098**, 27 (1991).
[3] L. Sokoloff, J. Neutrochem. **29**, 13 (1977).
[4] H. McIlwain, Biochem. J. **49**, 382 (1951).
[5] B. F. Levine, C. G. Bethea, and J. C. Campbell, Electron Lett. **20**, 596 (1984).
[6] B. F. Levine, C. G. Bethea, and J. C. Campbell, Electron Lett. **21**, 194 (1985).
[7] K. Kikuchi, T. Isoshima, and M. Yamada, Electron Lett. **25**, 1028 (1989).
[8] S. D. Personick, Bell Syst. Tech. J. **50**, 3075 (1971).
[9] R. J. McIntyre, IEEE Trans. Electron Devices **ED-19**, 703 (1972).
[10] J. Conradi, IEEE Trans. Electron Devices **ED-19**, 713 (1972).
[11] K. Hakomori and K. Kikuchi, Paper of Technical Group on Optical Quantum Electronics, IEICE of Japan, Paper OQE90-8 (1990).
[12] L.-Q. Li and L. M. Davis, Rev. Sci. Instrum. **64**, 1524 (1993).
[13] P. D. Townsend, J. G. Rarity, and P. R. Tapster, Electron Lett. **29**, 634 (1993).
[14] K. P. Ghiggino, M. R. Harris, and P. G. Spezzirri, Rev. Sci. Instrum. **63**, 2999 (1992).
[15] S. Cova, A. Lacaita, M. Ghioni, and G. Ripamonti, Opt. Lett. **14**, 1341 (1989).
[16] S. Cova, A. Lacaita, M. Ghioni, and G. Ripamonti, Rev. Sci. Instrum. **60**, 1104 (1989).
[17] J. G. Rarity, K. D. Ridley, and P. R. Tapster, Appl. Opt. **26**, 4616 (1987).
[18] R. G. W. Brown, K. D. Ridley, and J. G. Rarity, Appl. Opt. **25**, 4122 (1986).
[19] P. A. Ekstrom, J. Appl. Phys. **52**, 6974 (1981).
[20] A. Lacaita, S. Cova, and M. Ghioni, Rev. Sci. Instrum. **59**, 1115 (1988).
[21] G. Ripamonti and S. Cova, Electron Lett. **22**, 818 (1986).
[22] L. Stoppini, R. Buchs, and D. Muller, J. Neurosci. Methods **37**, 173 (1991).

Downloaded from http://pubs.aip.org/aip/rsi/article-pdf/66/4/2922/8809475/2922_1_online.pdf

Alidouble Inc. v. TSMC Alidouble Ex. 2009, p. 6